Published in final edited form as:
Eur J Nucl Med Mol Imaging. 2009 January ; 36(1): 94–103. doi:10.1007/s00259-008-0920-0.

Near-infrared optical imaging in glioblastoma xenograft with ligand targeting α3 integrin

Wenwu Xiao, **Nianhuan Yao**, **Li Peng**, **Ruiwu Liu**, and **Kit S Lam**
Division of Hematology & Oncology, Department of Internal Medicine, UC Davis Cancer Center, University of California Davis, 4501 X Street, Sacramento, California 95817

Abstract

Purpose—Patients with glioblastoma usually have a very poor prognosis. Even with a combination of radiotherapy plus temozolomide, the median survival of these patients is only 14.6 months. New treatment approaches to this cancer are needed. Our purpose is to develop new cell-surface binding ligands for glioblastoma cells, and use them as targeted imaging and therapeutic agents for this deadly disease.

Methods—One-bead one-compound combinatorial cyclic peptide libraries were screened with live human glioblastoma U-87MG cells. The binding affinity and targeting specificity of peptides identified were tested with *in vitro* experiments on cells and *in vivo*, and *ex vivo* experiments on U-87MG xegnograft mouse model.

Results—A cyclic peptide, LXY1, was identified and shown to be binding to the α3 integrin of U-87MG cells with moderately high affinity (Kd = 0.5+/−0.1 μM) and high specificity. Biotinylated LXY1, when complexed with streptavidin-Cy5.5 (SA-Cy5.5) conjugate, targeted both subcutaneous and orthotopic U-87MG xenograft implants in nude mice. The *in vivo* targeting specificity was further verified by strong inhibition of tumor uptake of LXY1-biotin-SA-Cy5.5 complex when intravenously injecting the animals with anti-α3 integrin antibody or excess unlabeled LXY1 prior to administrating the imaging probe. The smaller univalent LXY1-Cy5.5 conjugate (2279 Da) was found to have a faster accumulation in the U-87MG tumor and shorter retention time compared with the larger tetravalent LXY1-biotin-SA-Cy5.5 complex (~ 64 KDa).

Conclusions—Collectively, the data reveals that LXY1 has the potential to be developed into an effective imaging and therapeutic targeting agent for human glioblastoma.

Keywords

Combinatorial chemistry; one-bead one-compound peptide library; integrin; cancer targeting; glioblastoma; optical imaging

INTRODUCTION

Glioblastoma, the most common type of the primary brain tumor in adult, remains largely incurable, and surgical resection followed by radiation and chemotherapy has been shown to only slightly increase patient survival (1). There is a need for new approaches that can selectively target glioblastoma.

Corresponding author: Kit S Lam, Division of Hematology & Oncology, Department of Internal Medicine, UC Davis Cancer Center, University of California Davis, 4501 X Street, Sacramento, California 95817, USA. Phone: (916) 734-8012; FAX: (916) 734-7946; Kit.Lam@ucdmc.ucdavis.edu.

There is no conflict of interest for this manuscript

Integrins are expressed in most, if not all, cell types and have been implicated in a variety of biological processes including embryonic development, inflammation, thrombosis, tumor cell adhesion, metastasis, and adhesion mediated drug resistance (2). Integrins are transmembrane glycoprotein complexes of noncovalently linked α and β subunits. There are 8 known β subunits that combine with 18 α subunits in a defined manner to create more than 24 unique αβ heterodimers (3). It has been shown that brain tumor cells and proliferating tumor vasculature express high levels of the cell adhesion receptor αvβ3 and αvβ5 integrins *in vitro* and *in vivo* (4). Cyclic RGDfK peptide, a well-known ligand against αvβ3 integrin, has been widely used as an optical and radioimaging agent for solid tumors including glioblastoma when conjugated with fluorescent dye or radionuclide, respectively (5). Additionally, an extensive study on integrin expression patterns in normal and tumor tissues of the brain indicated that integrin α3β1 is the major integrin isotype expressed in glioma cells (6).

Through screening random one-bead one-compound (OBOC) cyclic peptide libraries, we previously identified a cyclic peptide motif, cDGXGXXc, to bind preferentially to ovarian cancer with high specificity against α3 integrin (7). We then synthesized and screened a cXGXGXXc focused-library against U-87MG human glioblastoma cells and identified a new cyclic peptide cdGLGBNc (named LXY1), wherein B stands for L-hydroxyproline, as an excellent ligand against U-87MG cells. In this paper we demonstrate that LXY1 binds to α3 integrin on brain tumors with high specificity and moderately high affinity utilizing *in vitro* binding experiments, as well as *in vivo* and *ex vivo* near infrared fluorescent (NIRF) optical imaging studies in xenograft models. The bio-distribution studies of two constructs of LXY1 imaging probes were also conducted.

MATERIALS AND METHODS

Materials

Rink amide MBHA resin (0.5 mmol/g), Fmoc-protected amino acids, and *N*-Hydroxybenzotriazole (HOBt) were purchased from GL Biochem (Shanghai, China). 1,3-Diisopropylcarbodiimide (DIC) was purchased from Advanced ChemTech (Louisville, KY). TentaGel S NH_2 resin (0.24mmol/g, 1% DVB cross-linked: 90μm) was purchased from Rapp Polymere (Tubingen, Germany). The other chemical reagents were purchased from Aldrich (Milwaukee, WI) and were of analytical grade. Anti-α3 and anti-β1 integrin antibodies were purchased from Chemicon (CHEMICON International, Inc). Human glioblastoma cell line U-87MG was obtained from American Type Culture Collection (Manassas,VA) and was maintained at 37°C in a humidified atmosphere containing 5% CO_2 in Eagle's Minimum Essential Medium and 10% fetal bovine serum (Omega Scientific, Inc).

Synthesis of the Cyclic Peptide cdGLGBNc (LXY1) on TentaGel Resins for On-bead Cell Binding Assay

Fmoc chemistry and HOBt/DIC coupling (8) was used to synthesize the cyclic peptide on beads. Three-fold molar excess of Fmoc- protected amino acids to resin were used for coupling. The reaction was monitored with the ninhydrin test. The Fmoc group was deprotected with 20% piperidine in DMF. After the side chain protecting groups were removed with trifluoroacetic acid (TFA) cocktail containing 82.5% TFA: 5% phenol: 5% thioanisole: 5% H_2O:2.5% triisopropylsilane (TIS), the peptide on beads were cyclized in 20% dimethyl sulfoxide (DMSO) (v:v) for 48 hr. Cyclization completion was confirmed by the Ellman test. The beads were then washed with water and stored in 75% ethanol (v:v).

Synthesis of LXY1 and Biotinylated Cyclic Peptide cdGLGBNc (LXY1) in Soluble Form

LXY1 and Biotinylated LXY1 (Figure 1a) were synthesized on Rink resin (loading 0.5mmol/g) using the above described Fmoc chemistry (8). cdGLGBNc-linker-linker-Biotin was

prepared on Rink resin using Fmoc-Lys(Alloc) as the first building block. After Alloc deprotection, Biotin was coupled to amino group at the ε position of Lys. Fmoc-linker (9) and Fmoc-amino acids were coupled to resin sequentially, followed by Fmoc deprotection. The peptides were finally cleaved from the Rink resins using TFA cocktail and then precipitated in cold diethyl ether. The crude peptides were cyclized in 50mM NH_4HCO_3 buffer (10) and then purified by preparative reverse-phase high performance liquid chromatography (RP-HPLC). Matrix-assisted laser desorption/ionization time of flight mass spectrometry (MALDI-TOF MS) was employed to verify the identity of the cyclic peptides.

Synthesis of LXY1-Cy5.5

Fmoc-cdGLGBNc-linker-linker-Lys(NH_2)-$CONH_2$ was first constructed on Rink resin using Fmoc chemistry (8). Then the compound was cleaved off the beads using TFA cocktail solution to give linear Fmoc-cdGLGBNc-linker-linker-Lys(NH_2)-$CONH_2$, and precipitated with diethyl ether. The crude peptide was added to 50mM NH_4HCO_3 followed by the addition of charcoal. The mixture was stirred until Ellman test was negative which indicated the completion of disulfide formation. After filtration, the solution was lypholized and purified by preparative RP-HPLC. To the cyclic peptide Fmoc-cdGLGBNc-linker-linker-Lys(NH_2)-$CONH_2$ in 0.1M $NaHCO_3$ (pH 8.3), Cy5.5-NHS was added. The mixture was mixed gently in dark overnight, followed by Fmoc deprotection with 20% piperidine. The final product (Figure 1b) was purified by preparative RP-HPLC, and verified by MALDI-TOF MS.

The Whole Cell Binding Assay

U-87MG cells adherent to the bottom of the T75 flask were trypsinized with 0.05% trypsin-EDTA and neutralized with growth medium. Floating cells were collected, spun down, and resuspended with 10ml growth medium in a 10cm Petri dish. Then LXY1-beads were washed sequentially with ethanol, water, and PBS. Thereafter the beads were incubated with suspended U-87MG cells, and the whole dish was kept shaking at a speed of 40 rpm inside an incubator at 37°C under 5% CO_2. The plate was then examined under an inverted microscope every 15 min.

Binding Affinity of LXY1 Peptide Detected by Flow Cytometry

U-87MG cells with 80–90% confluence were dissociated with 0.05% trypsin-EDTA and neutralized with growth medium. Each sample with 3×10^5 cells was incubated with biotinylated LXY1 at different concentrations in 50 μl PBS containing 10% FBS and 1 mM MnCl2 for 30 minutes on ice. To determine nonspecific binding, the samples were incubated with 10 μg anti-α3 integrin antibody for 30 min prior to incubation with biotinylated LXY1. After peptide incubation, each sample was washed three times with 1 ml PBS containing 1% FBS. Samples were incubated with 1:500 dilution of streptavidin-PE (1mg/mL) for 30 min on ice followed by washing once with 1 ml PBS containing 1% FBS. Finally the samples were analyzed with flow cytometry (Coulter XL-MCL), and the mean fluorescence intensity (MFI) was determined. The apparent Kd was calculated using Graph Prism software (www.graphpad.com).

Fluorescence Microscopy

Sample preparation was the same as above described for flow cytometry studies. Instead of running the cells through a flow cytometer, the cells were examined under a fluorescent microscope. To conduct the blocking experiment, unlabeled LXY1 peptide and anti-α3 integrin antibody were incubated with the cells together with the biotinylated LXY1. After the last wash, the cell pellet was resuspended in 100 μL PBS and loaded into the container for Cytospin centrifuge (Cytospin3, SHANDON). The cells were spun down onto slides at 2000 rpm for 2

min and mounted by the fluorescence mount solution including DAPI. Thereafter the cells were covered by cover slip and examined under a fluorescence microscope (IX81, Olympus).

Tumor Xenografts

Animal studies were performed according to a protocol approved by IACUC of the University of California, Davis. Female athymic nude mice (nu/nu), obtained from Harlan (Indianapolis, IN) at 5–6 weeks of age, were injected subcutaneously in the right flank with 5×10^6 U-87MG glioblastoma cells suspended in 200 μl PBS. In some mice, 5×10^6 K562 chronic myeloid leukemia cells were implanted in the opposite side as a negative control. For the orthotopic implantation, 2.5×10^5 cells in 5 μL PBS were injected into the right striatum area of the mouse with the aid of a mouse stereotactic instrument (Stoelting Co.) When the subcutaneous tumors reached 0.5 to 1.0 cm in diameter or 21–28 days after implantation, at that time the mean size of orthotopic tumors was 0.2 to 0.5 cm in diameter, the tumor-bearing mice were subjected to in vivo and ex vivo imaging studies.

Near Infrared Fluorescence Imaging Studies

Tetravalent LXY1-biotin-streptavidin complex (1.8 nmole), prepared by mixing 7.2 nmole of biotinylated LXY1 with 1.8 nmole of streptavidin-Cy5.5 in PBS overnight at 4°C or 7.2 nmole of univalent LXY1-Cy5.5 conjugate was injected via the tail vein in the mouse anesthetized by injection of 30 μL Nembutal (50mg/ml) before imaging. To conduct blocking experiments, 3.6 μmole of LXY1 or 20 μg anti-α3 integrin antibody was injected via tail vein 1 hr prior to injection of the optical probe. Animals were placed on a sheet of transparency in the supine position. Images were acquired with a Kodak IS2000MM Image station (Rochester, NY) with excitation filter 625/20 band pass, emission filter 700WA/35 band pass, and 150 W quartz halogen lamp light source set to maximum. Images were captured with a CCD camera set at F stop=0, FOV=150, and FP=0. Data were collected at different time points and analyzed using the Kodak ID 3.6 software by drawing the region of interest (ROI) on the imaged mouse. In *ex vivo* imaging, the mice were sacrificed and organs excised for imaging.

Data Processing and Statistics

For determination of tumor contrast, we calculated mean fluorescence intensities of the tumor area and of the normal tissue area by means of the region-of–interest function using Kodak 1D Image Analysis Software (Kodak). All the data are shown as mean +/- s.d. of n independent measurements. Student's *t*-test was used for statistical analysis of *ex vivo* imaging intensity. Statistical significance was indicated by $P<0.05$ and $P<0.001$.

Results

LXY1 TentaGel Beads Binding with U-87MG Cells

LXY1 peptide was resynthesized on TentaGel beads. When U-87MG cells were incubated with the LXY1-beads, the beads were entirely covered by a monolayer of cells within 30 min (Figure 2a), indicating that LXY1 peptide binds strong to U-87MG cells.

Binding affinity of LXY1 against U-87MG Cells

We used flow cytometry to determine the apparent binding affinity of LXY1 peptide against U-87MG cells. U-87MG cells were treated with or without 10μg anti-α3 integrin antibody for 30 min prior to incubation with biotinylated LXY1. After thorough washing, the cells were mixed with streptavidin-PE for 30 min, washed and then analyzed by flow cytometry. The mean fluorescent intensity of the group pre-treated with antibody is depicted as non-specific binding of the peptide to the cells, and that of the group treated with only peptides is defined as total binding. By subtracting non-specific binding from total binding at various

concentrations of peptide, the apparent Kd for specific binding of LXY1 was calculated to be 0.5+/- 0.1μM (Figure 2b).

Fluorescent Staining of U-87MG Cells with LXY1 Peptide

The U-87MG cells were incubated with biotinylated LXY1 for 30 min, washed 3 times with PBS, incubated with streptavidin-Alexa488 for 30 min, washed 1 time with PBS and then examined under a fluorescent microscope. For the blocking experiments, unlabeled LXY1 peptide or anti-α3 antibody was added prior to introduction of biotinylated LXY1. Figure 3a clearly demonstrates that cell staining by biotinylated LXY1 was almost completely abolished by either unlabeled LXY1 or anti-α3 antibody, indicating that LXY1 peptide binds specifically to the α3-integrin of U-87MG glioblastoma cells.

In vivo and *Ex vivo* Near-Infrared Optical Imaging of Subcutaneous and Orthotopic U-87MG Xenograft Implant in Nude Mice

To maintain the 4:1 molar ratio of biotin:streptavidin, 7.2 nmole biotinylated LXY1 was mixed with 1.8 nmole of streptavidin-Cy5.5 (based on streptavidin) to form a tetravalent complex prior to injection into the mice via the tail vein. In the bio-distribution study, *ex vivo* NIRF imaging was conducted at 30min, 4 hr, 6 hr, 24 hr, 48 hr after injection. The accumulation of the tetravalent optical probe in U-87MG tumor peaked at around 4 hr and then decreased gradually, but with over 80% of the peak level retained in the tumor even at 48 hr. Renal uptake of the tetravalent optical probe followed similar pharmacokinetics. NIRF probe uptake into the skin and liver was also seen but was significantly lower than that of the tumor and the kidneys (Figure 6a). To determine tumor targeting specificity, U-87MG cells were implanted subcutaneously to one side of the nude mouse. K562 chronic myeloid leukemia cells (expressing α5β1 integrin) were injected into the opposite side of the same nude mouse as a negative control. After the tumors reached 0.5 to 1.0 cm in diameter, the mice bearing both U-87MG and K562 tumors were injected via tail vein with 1.8 nmole of the tetravalent LXY1-biotin-SA-Cy5.5 complex. Four hours post-injection, the animals were scanned with the Kodak Imaging Station. Figure 3b clearly shows that uptake of the NIRF probe into U-87MG tumor was statistically significant higher than that of K562.

For the *in vivo* blocking experiments, 3.6 μmole unlabeled LXY1 peptide or 20 μg (~0.13 nmole) anti-α3 integrin antibody was administered i.v. one hour prior to the administration of the tetravalent complex. *Ex vivo* organs and tumor imaging studies (Figure 4a & 4b) clearly demonstrate that uptake of the NIRF probe by U-87MG tumor was much higher than that of K562 tumor ($P<0.001$). Furthermore, uptake of the imaging probe by U-87MG tumor was almost completely blocked by prior injection with either excess unlabeled LXY1 ($P<0.001$) or anti-α3 integrin antibody ($P<0.001$). These results further demonstrate that LXY1 is highly specific against the α3 integrin receptor on U-87MG tumor. Kidney uptake of the NIRF probe was significant in these studies and was not blocked by unlabeled LXY1 nor anti-α3 integrin antibody. This is not unexpected as it has been reported in the literature that streptavidin alone does bind to kidney when administered intravenously. Uptake of the optical probe in other normal organs was moderate in the skin and liver but very low in other organs.

We have also performed NIRF imaging experiments in nude mice bearing both subcutaneous and orthotopic U-87MG implants. *Ex vivo* imaging studies shown in Figure 5a & 5b clearly demonstrate that uptake of the NIRF probe into the subcutaneous tumor implant was very high while uptake into the normal organs was relatively low with the kidneys excepted. Very importantly, uptake of the imaging probe by the orthotopic U-87MG implant in the right brain was also much higher than that of the normal brain tissue ($P<0.001$), although it was lower than that of the subcutaneous U-87MG tumor ($P<0.05$).

We have also conducted *in vivo* imaging studies in nude mice bearing U-87MG tumor with the much smaller univalent LXY1-Cy5.5 conjugate. 7.2 nmole of LXY1-Cy5.5 was injected via tail vein and *ex vivo* imaging was conducted at 15min, 1hr, 2hr, 4hr and 24hr post-injection. Figure 6b shows that near infrared signal in both the tumor and kidneys peaked within 15 min after i.v. injection of the optical probe, followed by a rapid clearance to approximately 50% of the peak level by 2 hr, and then a much slower clearing phase over the next 22 hr. This biodistribution result is very different from that obtained by the larger tetravalent conjugate, in which tumor and kidney uptake peaked at 4 hr followed by a very slow drop over the next 44 hr (Figure 6a).

Discussion

The OBOC combinatorial library method was developed over a decade ago (11). Thousands to millions of compound-beads can be generated and screened rapidly. Each OBOC library compound-bead displays only one chemical entity. One major advantage of OBOC method over the phage-display method is that D-amino acids, unnatural amino acids, and organic moieties can be easily incorporated into the construction of the OBOC libraries, rendering the identified ligands containing such building blocks more resistant to proteolysis. The phage-display peptide library method, on the other hand, is generally limited to only L-amino acids, and therefore the peptides are more susceptible to proteolysis (12). Using OBOC combinational approaches, we have previously reported the identification of peptide and peptidomimetic ligands against cell surface receptors on several tumor types, such as α6β1 integrin of prostate cancer (13), α4β1 integrin of malignant lymphoma (14,15), α3β1 integrin of non-small cell lung cancer (16) and ovarian cancer (7). The cD/NGXGXXc peptide motifs that we previously identified were found to bind α3β1 integrin of lung and ovarian cancers (7,16). Based on these results, a focused library cXGXGXXc was synthesized and screened against ovarian cancer cell lines (7). Cyclic peptide OA02 or cdG-Hci-GPQc (Hci: homocitrulline) was developed and demonstrated to have good *in vivo* targeting properties both in optical (17) and PET imaging (12) of ovarian cancer xenografts. α3β1 integrin is expressed widely in normal organs and tumor tissues. It plays an important role in normal lung, kidney, and epithelial development, as well as neuronal migration during cerebral cortical development (18–21). It also plays a crucial role in tumor cell adhesion, migration, invasion, and metastasis (22–25). Many different kinds of epithelial tumors such as ovarian cancer, melanoma, and glioblastoma over express α3β1 integrin. Through screening focused OBOC libraries and retesting the positive ligands against a series of α3β1 integrin expressing tumor cells, we noticed that the binding profile of these ligands against the different cell lines varies somewhat despite the ligands having the same cdGXGXXc motif (12). We believe all these ligands do bind to α3 integrin because cell binding to such beads can be blocked by anti-α3 antibody. Our hypothesis is that the α3 integrins expressed on each of these cancer cell lines may have somewhat different conformation or states and are therefore different from α3 integrins expressed on normal cells. The hypothesis is supported by (i) our observation that LLP2A, the high affinity and high specificity peptidomimetic ligand against B-and T-lymphoma cells, binds strongly to the activated α4β1 integrin on these malignant cells, moderately to α4β1 integrin of normal peripheral blood mononuclear cells activated by Mn^{2+},but not to unactivated α4β1 integrin present on the resting lymphoid cells isolated from normal peripheral blood (14), and (ii) the *ex vivo* imaging data (Figure 4a) shows excellent uptake in subcutaneous tumor implant but much lower in many normal organs which also express α3 integrin.

We screened the focused cXGXGXXc library against glioblastoma cell line (U-87MG) and identified LXY1, which was found to bind to U-87MG cells at a moderately high affinity and with high specificity to α3 integrin receptor on the cell surface. Unlike anti-α3 integrin antibody, anti-β1 integrin antibody was not able to block the binding of U-87MG cells to

LXY1-bead. A negative result, however, cannot rule out that β1 is not involved in the binding of LXY1 to U-87MG cells.

Although optical imaging may not be useful as a non-invasive imaging agent for clinical glioblastoma, it is extremely useful as a preclinical imaging tool to evaluate or screen tumor targeting ligands. Optical imaging is technically easy to do, non-radioactive, and relatively inexpensive. We therefore can use this approach to determine the cancer-targeting potential of a number of ligands; and based on the optical imaging result, we can then select a few ligands for further development into *in vivo* radio-targeting and chemo-targeting agents. In this report, we first used the larger tetravalent LXY1-biotin-SA-Cy5.5 complex (~64 KDa) as the NIRF optical imaging probe in a xenograft model. Uptake of the conjugate into the subcutaneous tumor implant was very high, as were the kidneys. High renal uptake of the conjugate is not unexpected as streptavidin is known to bind to kidney (26). Uptake of the conjugate to other normal organs, however, was very low (Figure 6a). For brain cancer targeting agents, we need to demonstrate that these compounds can be effectively delivered to the tumors within the brain. To achieve this, we performed NIRF optical imaging studies in nude mice that have received both subcutaneous and orthotopic U-87MG implants. As expected, uptake of LXY1-biotin-streptavidin-Cy5.5 conjugate into the subcutaneous implant was very high, and uptake into the kidneys was moderately high. More importantly, LXY1 uptake into the orthotopic implant was also very significant (Figure 5a & 5b). This observation, however, does not necessarily mean that LXY1-biotin-streptavidin-Cy5.5 conjugate could penetrate the blood brain barrier. More than likely, the blood brain barrier was compromised at the tumor site (27) and therefore allowed LXY1 conjugate to reach the orthotopic target xenograft.

In addition to testing the large tetravalent LXY1-Biotin-SA-Cy5.5 complex as an imaging probe, we also evaluated the tumor targeting capability of the much smaller univalent LXY1-Cy5.5 conjugate (2279 daltons). The bio-distribution studies showed that LXY1-Cy5.5 uptake in the subcutaneous U-87MG tumor peaked within 15 min after i.v. injection and was washed out quickly (within 4 hr). The pharmacokinetic profile of this small conjugate was very different from that of LXY1-Bio-SA-Cy5.5, in which the uptake of the larger probe peaked at around 4 hr with very slow wash out even after 48 hr. This can in part be explained by the difference in size and valency of the conjugates. The prolonged retention of the streptavidin complex in the kidney is probably due to the non-specific binding of streptavidin to the kidney (26). Whether LXY1 directly binds to the kidney or not is unclear at this time as Cy5.5 itself may also bind to the kidneys. Preliminary data in our laboratory showed that LLP2A, the lymphoma targeting ligand, when conjugated to the metal chelator CB-TE2A and complexed with ^{64}Cu can obviate renal uptake (data not shown), suggesting that LLP2A does not bind to the renal cells even though LLP2A-biotin-SA-Alexa680 complex does (14). We plan to synthesize LXY1-CB-TE2A conjugate and label it with ^{64}Cu for PET imaging studies. This study will enable us to determine if LXY1 binds to the kidney or not. It will also allow more precise biodistribution studies and clarify brain uptake levels of the new tracer in functional and impaired blood brain barrier. Eventually direct conjugation of LXY1 with radionuclides without streptavidin will be developed. The smaller univalent conjugation may be more suitable to be used as the image radiotracer because of its quicker washout and shorter retention time. However the multivalent conjugation with longer retention time but with lower kidney uptake will be the future direction for conjugation optimization. This can be accomplished by using branched polyethylene glycol instead of streptavidin as the scaffold for LXY1 conjugation. Should ^{64}Cu-labeled LXY1-CB-TE2A conjugate target orthotopic and subcutaneous glioblastoma with high efficiency and specificity, and with low uptake to liver or kidney, the same ligand-metal chelate can be loaded with ^{67}Cu for cancer radiotherapy. If kidney uptake remains high with the small univalent radioconjugate, we shall prepare larger univalent or tetravalent radioconjugates by ligating LXY1 and CB-TE2A to an inert multi-branched polyethylene glycol platform (50,000 daltons)

that is excluded from filitration through the glomeruli in the kidneys. Alternative route of administration of the radioconjugate is intralesional injection.

In summary, we have demonstrated that LXY1 cyclic peptide, discovered through OBOC combinatorial library methods, can bind U-87MG brain tumor cells with high specificity and moderately high affinity. We have further shown that LXY1 can target both subcutaneous and orthotopic U-87MG implants with high specificity. We have also established the difference in the bio-distribution profiles of LXY1-Bio-SA-Cy5.5 and LXY1-Cy5.5. Work is currently underway in our laboratory to develop LXY1 into an effective vehicle for the delivery of radiotherapeutic and chemotherapeutic drugs to the glioblastoma.

Acknowledgments

This work was supported by the National Institutes of Health (R33CA-86364, R33CA-99136, U19CA113298, and P50CA097257). We like to thank Ms. Mary Saunders and Mr. Joel Kugelmass for editorial assistance.

Abbreviations

Standard single letter amino acids are used for all natural L-amino acids, lower case

c	D-cysteine
B	L-hydroxyl-proline
X	random amino acids
Hci	homocitrulline
HOBt	1-Hydroxybenzotriazole
DIC	1,3-Diisopropylcarbodiimide
TFA	Trifluoroacetic acid
TIS	Triisopropylsilane
EDTA	ethylenediaminetetraacetic acid
PE	Phycoerythrin
DAPI	4',6-diamidino-2-phenylindole
IACUC	Institutional Animal Care and Use Committee
FBS	fetal bovine serum
PBS	phosphate-buffered saline

References

1. Stupp RMW, van den Bent MJ, et al. Radiotherapy plus concomitant and adjuvant temozolomide for glioblastoma. N Engl J Med 2005;352(10):987–96. [PubMed: 15758009]
2. Hynes RO. Metastatic potential: generic predisposition of the primary tumor or rare, metastatic variants-or both? Cell 2003;113(7):821–3. [PubMed: 12837240]
3. Hynes RO. Integrins: bidirectional, allosteric signaling machines. Cell 2002;110(6):673–87. [PubMed: 12297042]
4. Taga T, Suzuki A, Gonzalez-Gomez I, et al. Alpha v-Integrin antagonist EMD 121974 induces apoptosis in brain tumor cells growing on vitronectin and tenascin. Int J Cancer 2002;98(5):690–7. [PubMed: 11920637]
5. Chen X, Conti PS, Moats RA. *In vivo* near-infrared fluorescence imaging of integrin alphavbeta3 in brain tumor xenografts. Cancer Res 2004;64(21):8009–14. [PubMed: 15520209]

6. Paulus W, Baur I, Schuppan D, Roggendorf W. Characterization of integrin receptors in normal and neoplastic human brain. Am J Pathol 1993;143(1):154–63. [PubMed: 8317546]
7. Aina OH, Marik J, Liu R, Lau DH, Lam KS. Identification of novel targeting peptides for human ovarian cancer cells using "one-bead one-compound" combinatorial libraries. Mol Cancer Ther 2005;4 (5):806–13. [PubMed: 15897245]
8. Liu, G.; Lam, KS. One-bead one compound combinatorial library method. In: H F, editor. Combinatorial chemistry. Oxford University Press; New York: 2000. p. 33-49.
9. Song A, Wang X, Zhang J, Marik J, Lebrilla CB, Lam KS. Synthesis of hydrophilic and flexible linkers for peptide derivatization in solid phase. Bioorg Med Chem Lett 2004;14(1):161–5. [PubMed: 14684320]
10. Volkmer-Engert R, Landgraf C, Schneider-Mergener J. Charcoal surface -assisted catalysis of intramolecular disulfide bond formation in peptides. J Pept Res 1998;51(5):365–9. [PubMed: 9606016]
11. Lam KS, Salmon SE, Hersh EM, Hruby VJ, Kazmierski WM, Knapp RJ. A new type of synthetic peptide library for identifying ligand-binding activity. Nature 1991;354(6348):82–4. [PubMed: 1944576]
12. Aina OH, Liu R, Sutcliffe JL, Marik J, Pan CX, Lam KS. From combinatorial chemistry to cancer-targeting peptides. Mol Pharm 2007;4(5):631–51. [PubMed: 17880166]
13. DeRoock IB, Pennington ME, Sroka TC, et al. Synthetic peptides inhibit adhesion of human tumor cells to extracellular matrix proteins. Cancer Res 2001;61(8):3308–13. [PubMed: 11309285]
14. Peng L, Liu R, Marik J, Wang X, Takada Y, Lam KS. Combinatorial chemistry identifies high-affinity peptidomimetics against alpha4beta1 integrin for in vivo tumor imaging. Nat Chem Biol 2006;2(7): 381–9. [PubMed: 16767086]
15. Peng L, Liu R, Andrei M, Xiao W, Lam KS. *In vivo* optical imaging of human lymphoma xenograft using a library-derived peptidomimetic against alpha4beta1 integrin. Mol Cancer Ther 2008;7(2): 432–7. [PubMed: 18245670]
16. Lau D, Guo L, Liu R, Marik J, Lam K. Peptide ligands targeting integrin alpha3beta1 in non-small cell lung cancer. Lung Cancer 2006;52(3):291–7. [PubMed: 16635537]
17. Aina OH, Marik J, Gandour-Edwards R, Lam KS. Near-infrared optical imaging of ovarian cancer xenografts with novel alpha 3-integrin binding peptide "OA02". Mol Imaging 2005;4(4):439–47. [PubMed: 16285906]
18. Schmid RS, Shelton S, Stanco A, Yokota Y, Kreidberg JA, Anton ES. Alpha3 beta1 integrin modulates neuronal migration and placement during early stages of cerebral cortical development. Development 2004;131(24):6023–31. [PubMed: 15537685]
19. Kreidberg JA, Symons JM. Integrins in kidney development, function, and disease. Am J Physiol Renal Physiol 2000;279(2):F233–42. [PubMed: 10919841]
20. Wang Z, Symons JM, Goldstein SL, McDonald A, Miner JH, Kreidberg JA. Alpha3 beta1 integrin regulates epithelial cytoskeletal organization. J Cell Sci 1999;112(Pt 17):2925–35. [PubMed: 10444387]
21. DiPersio CM, Hodivala-Dilke KM, Jaenisch R, Kreidberg JA, Hynes RO. Alpha3beta1 Integrin is required for normal development of the epidermal basement membrane. J Cell Biol 1997;137(3): 729–42. [PubMed: 9151677]
22. Morini M, Mottolese M, Ferrari N, et al. The alpha 3 beta 1 integrin is associated with mammary carcinoma cell metastasis, invasion, and gelatinase B (MMP-9) activity. Int J Cancer 2000;87(3): 336–42. [PubMed: 10897037]
23. Coopman PJ, Thomas DM, Gehlsen KR, Mueller SC. Integrin alpha 3 beta 1 participates in the phagocytosis of extracellular matrix molecules by human breast cancer cells. Mol Biol Cell 1996;7 (11):1789–804. [PubMed: 8930900]
24. Van der Pluijm, Vloedgraven H, Papapoulos S, et al. Attachment characteristics and involvement of integrins in adhesion of breast cancer cell lines to extracellular bone matrix components. Lab Invest 1997;77(6):665–75. [PubMed: 9426405]
25. Kiefer JA, Farach-Carson MC. Type I collagen-mediated proliferation of PC3 prostate carcinoma cell line: implications for enhanced growth in the bone microenvironment. Matrix Biol 2001;20(7): 429–37. [PubMed: 11691583]

26. Wilbur DS, Hamlin DK, Sanderson J, Lin Y. Streptavidin in antibody pretargeting. 4. Site-directed mutation provides evidence that both arginine and lysine residues are involved in kidney localization. Bioconjug Chem 2004;15(6):1454–63. [PubMed: 15546215]

27. Deeken JF, Löscher W. The blood-brain barrier and cancer: transporters, treatment, and Trojan horses. Clin Cancer Res 2007;13(6):1663–74. [PubMed: 17363519]

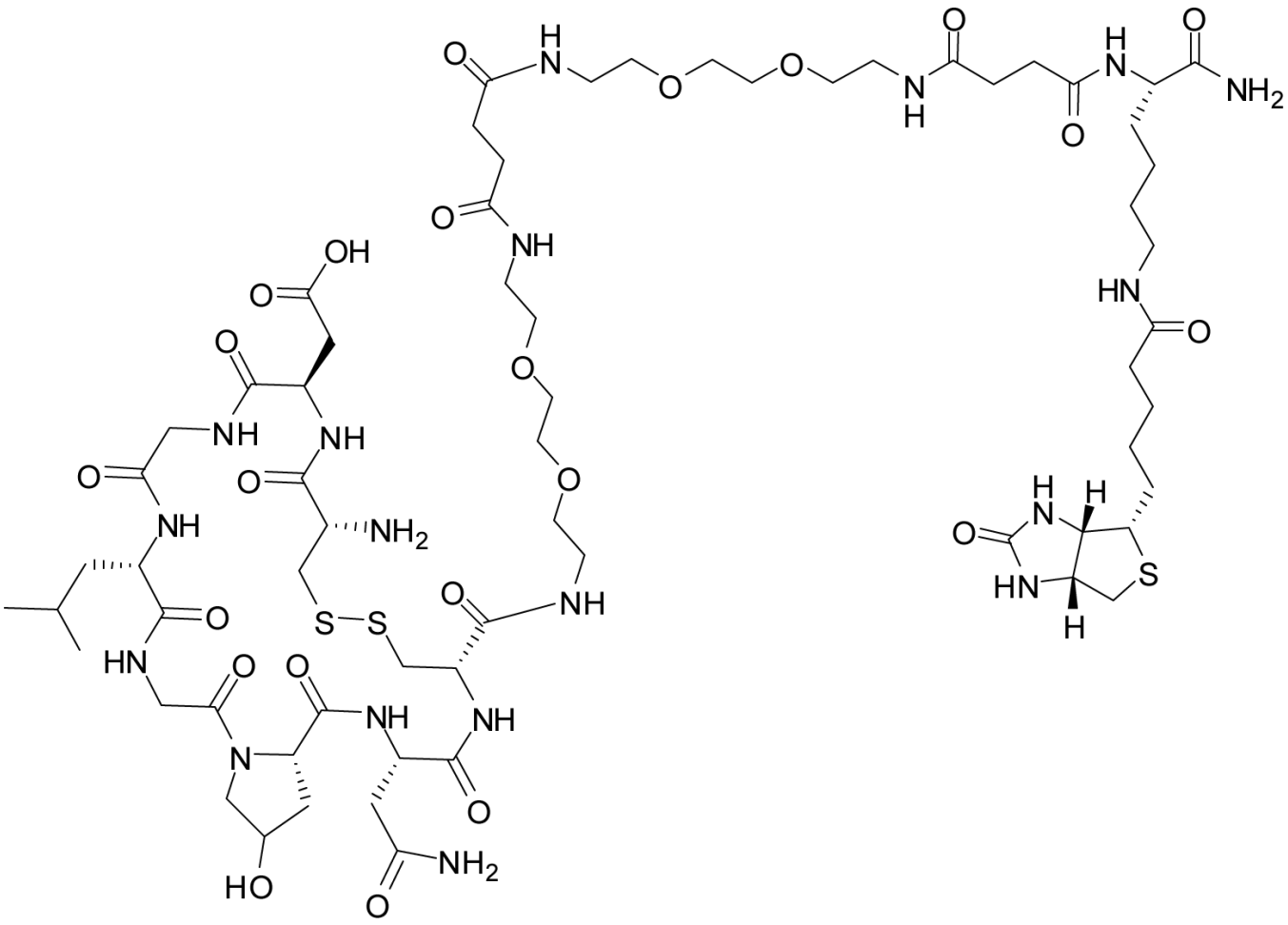

Figure 1a.
Chemical structure of the biotinylated LXY1. Two hydrophilic linkers were inserted between Lys(biotin) and LXY1.

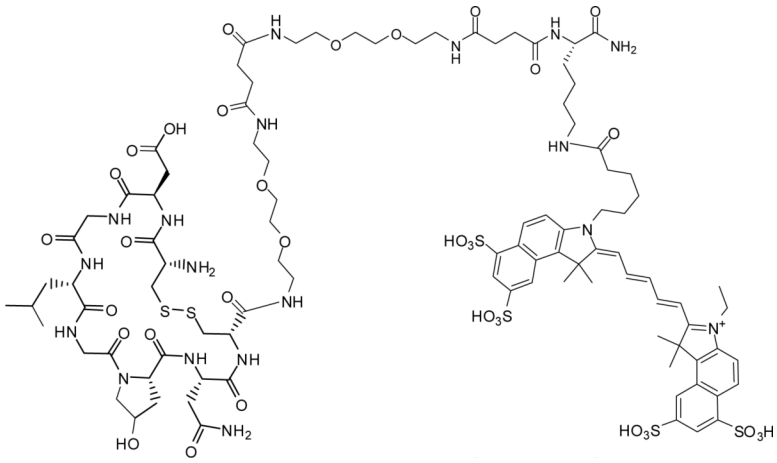

Figure 1b.
Chemical structure of LXY1-Cy5.5

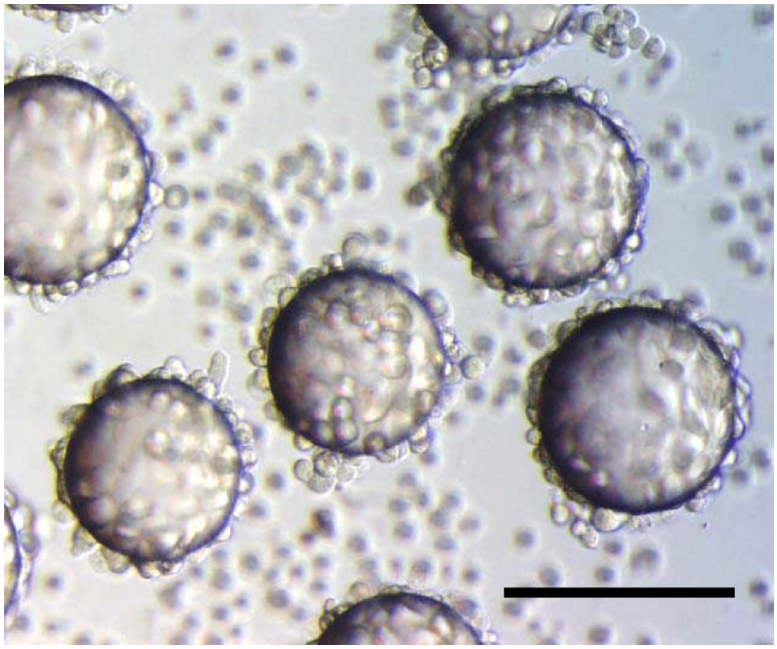

Figure 2a.
Whole Cell Binding Assay: U-87 MG cells bind strongly to the LXY1-beads in 30 min. Scale bar=100μm

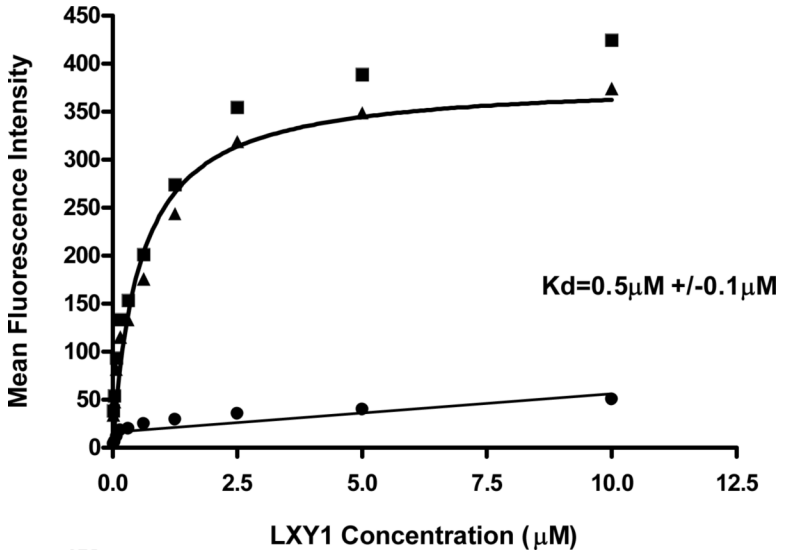

Figure 2b.

Determination of binding affinity by flow cytometry. Biotinylated LXY1 followed by Streptavidin-PE was mixed with U-87 MG (3×10^5 cells / sample) prior to flow cytometry analysis and mean fluorescent signal was determined. (■): total binding; (•): nonspecific binding (after blocking by 10 μg anti-α3 antibody); (▲): specific binding obtained by subtracting nonspecific binding from total binding. The solid line through the specific binding data represent nonlinear regression fits of data to the equation Y=Bmax*X/(Kd+X), where Kd is the apparent dissociation constant of the ligand.

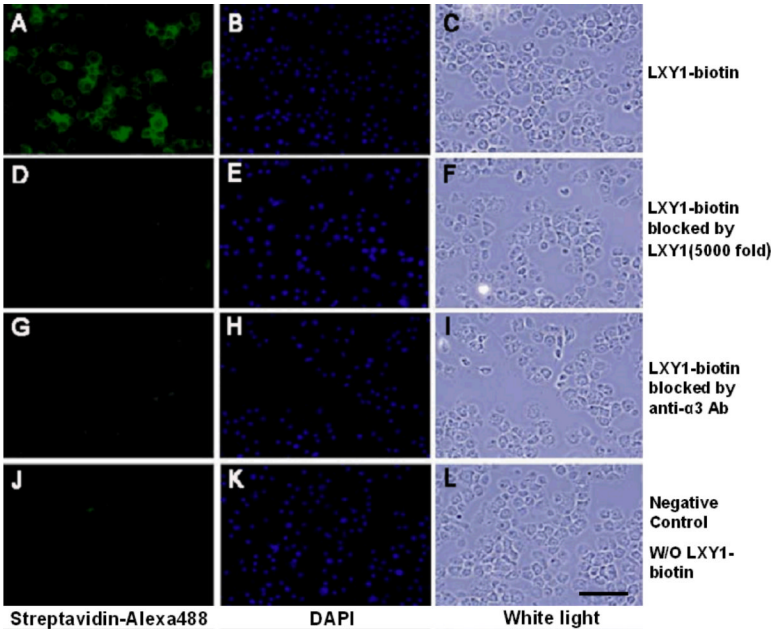

Figure 3a.

Fluorescent microscopy of U-87MG cells stained with biotinylated LXY1 followed by streptavidin-Alexa488; nuclei were counterstained by DAPI. Strong staining of U-87 MG cell with LXY1-biotin was observed (A). The fluorescent signal was almost completely abolished by co-incubation with excess unlabeled LXY1 (D) or anti-α3 integrin monoclonal antibody (clone P1B5) (G). Scale bar =100μm

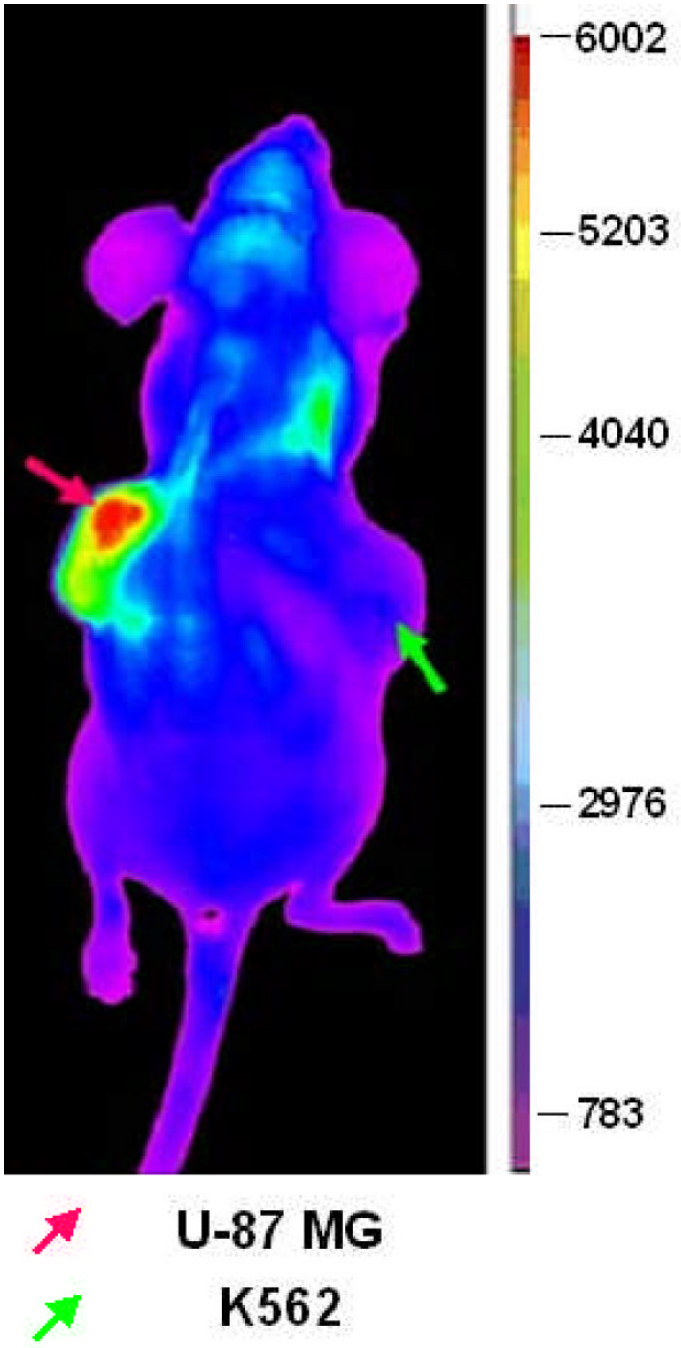

Figure 3b.
Near infrared fluorescent *in vivo* imaging of mouse bearing subcutaneous U-87MG tumor. Tetravalent LXY1-biotin-SA-Cy5.5 imaging complex accumulated in the U-87MG tumor (red arrow), but not in K562 tumor (green arrow).

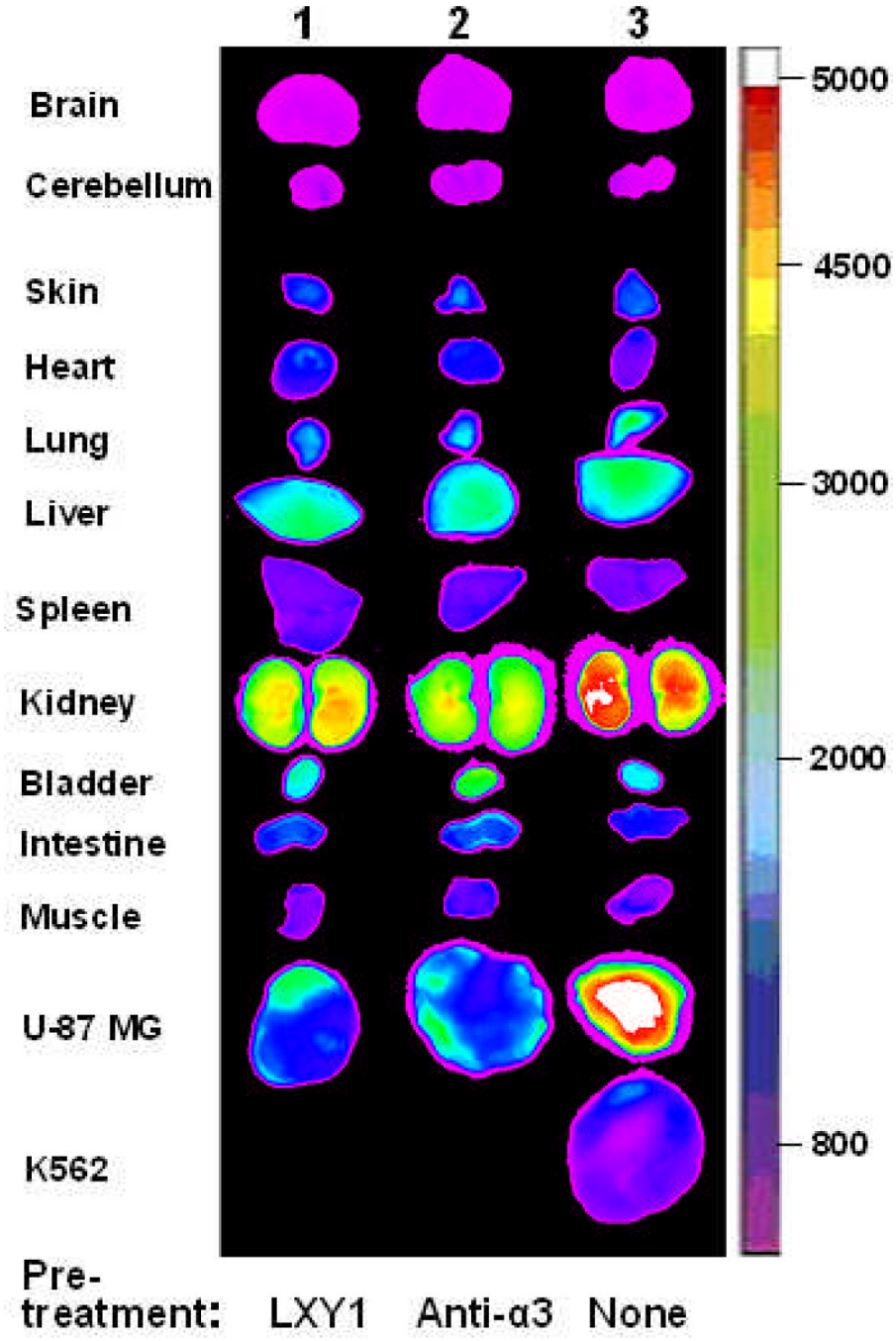

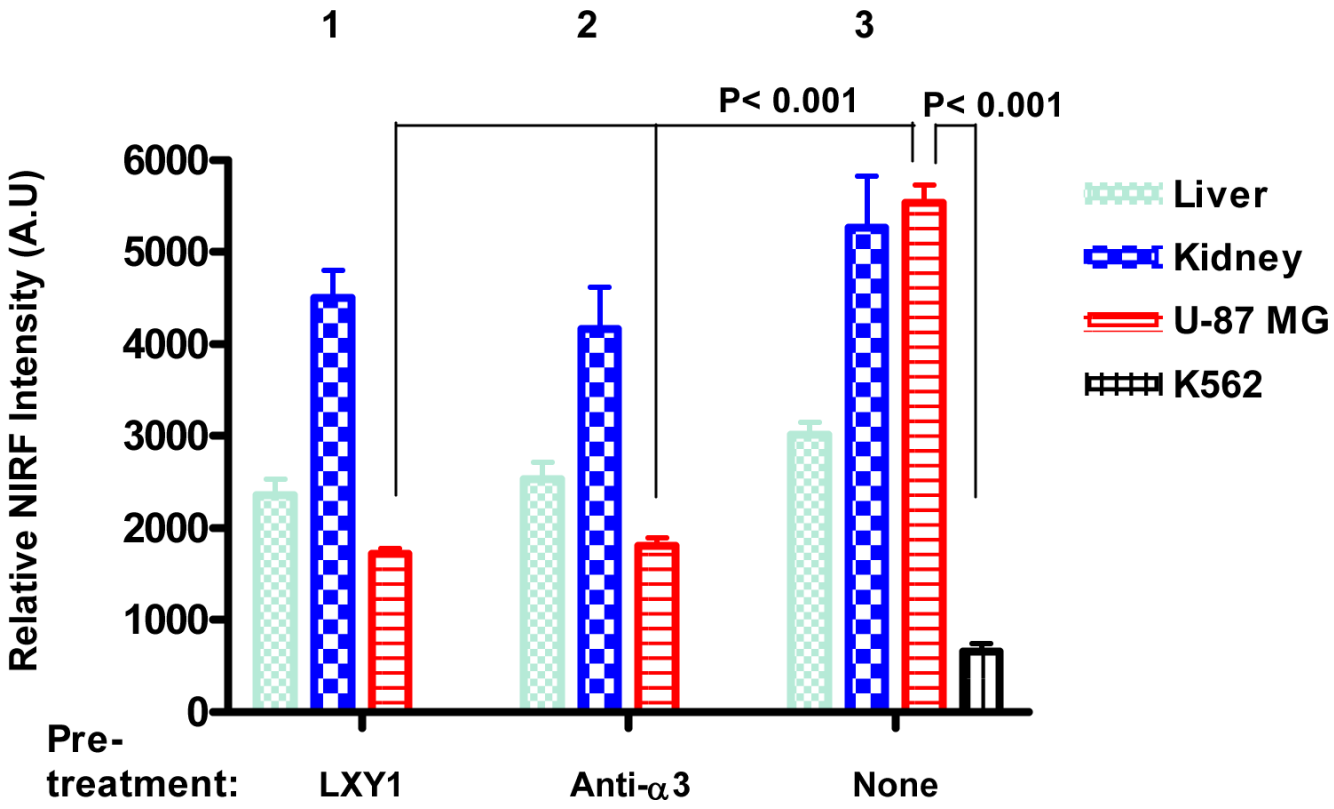

Figure 4a.

Near infrared *ex vivo* imaging of mice bearing subcutaneous U-87 MG tumor and the blocking effect of unlabeled peptide and anti-α3 integrin antibody. Group 1, free LXY1 was given 1 hr prior to LXY1-biotin-SA-Cy5.5 injection. Group 2, anti-α3 integrin antibody was given 1 hr prior to LXY1-biotin-SA-Cy5.5 injection. Group 3, mice bearing U-87 MG and K562 tumor was injected with LXY1-biotin-SA-Cy5.5 without blocking agent. Quantitative analysis is shown as Figure 4b. Compared with Group 3 treated with LXY1-biotin-SA-Cy5.5, the signals in U-87 MG in Group 1 and 2 decreased significantly (n=3, P<0.001). And the peptide imaging complex LXY1-biotin-SA-Cy5.5 significantly accumulated in U-87 MG tumor, but not in K562 tumor in Group 3 (n=3, P<0.001). There were also some NIRF uptake in the kidney and liver in all groups.

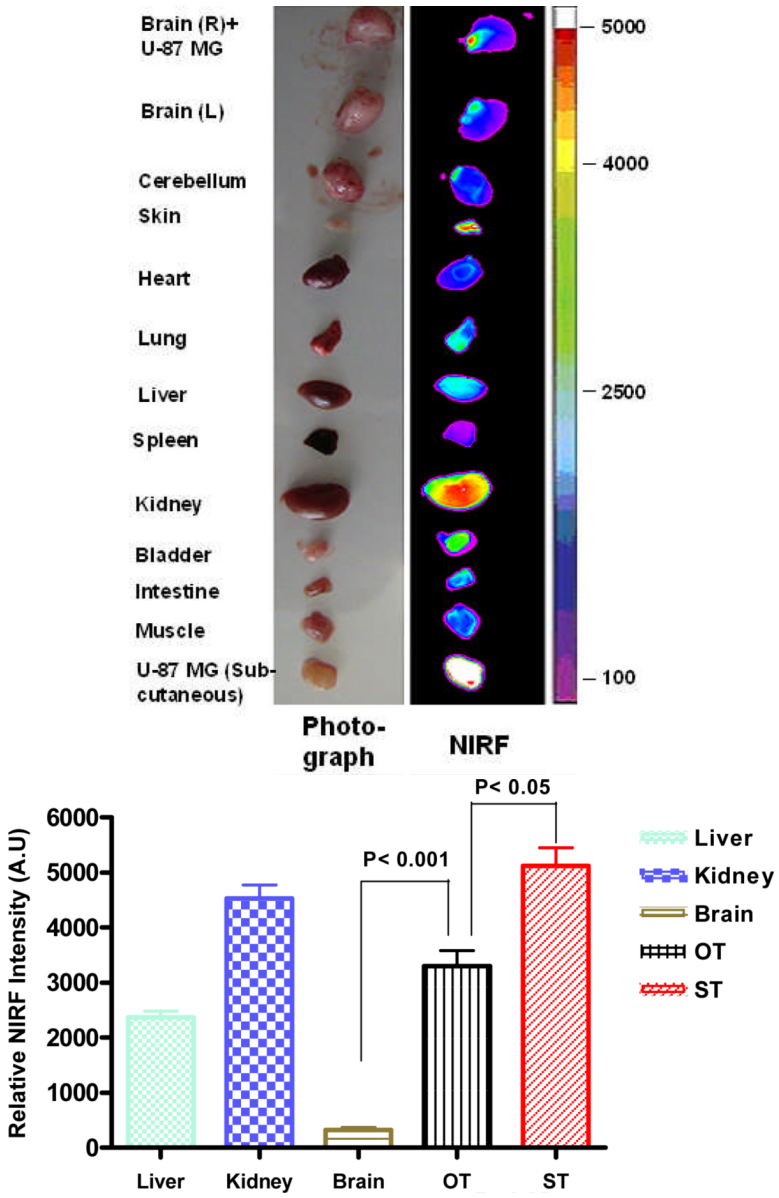

Figure 5a.

Near infrared fluorescent *ex vivo* imaging of mice bearing orthotopic and subcutaneous U-87MG tumor. NIRF signal of tumor and organs indicates that the imaging complex LXY1-biotin-SA-Cy5.5 accumulated in both orthotopic tumor (OT) and subcutaneous tumor (ST). Quantitative analysis of NIRF uptake is shown in Figure 5b. NIRF signal in OT was significantly higher than that in normal brain tissue (n=3, $p<0.001$) but lower than that in ST (n=3, $p<0.001$). Kidney uptake was as high as tumor uptake and liver uptake was significant.

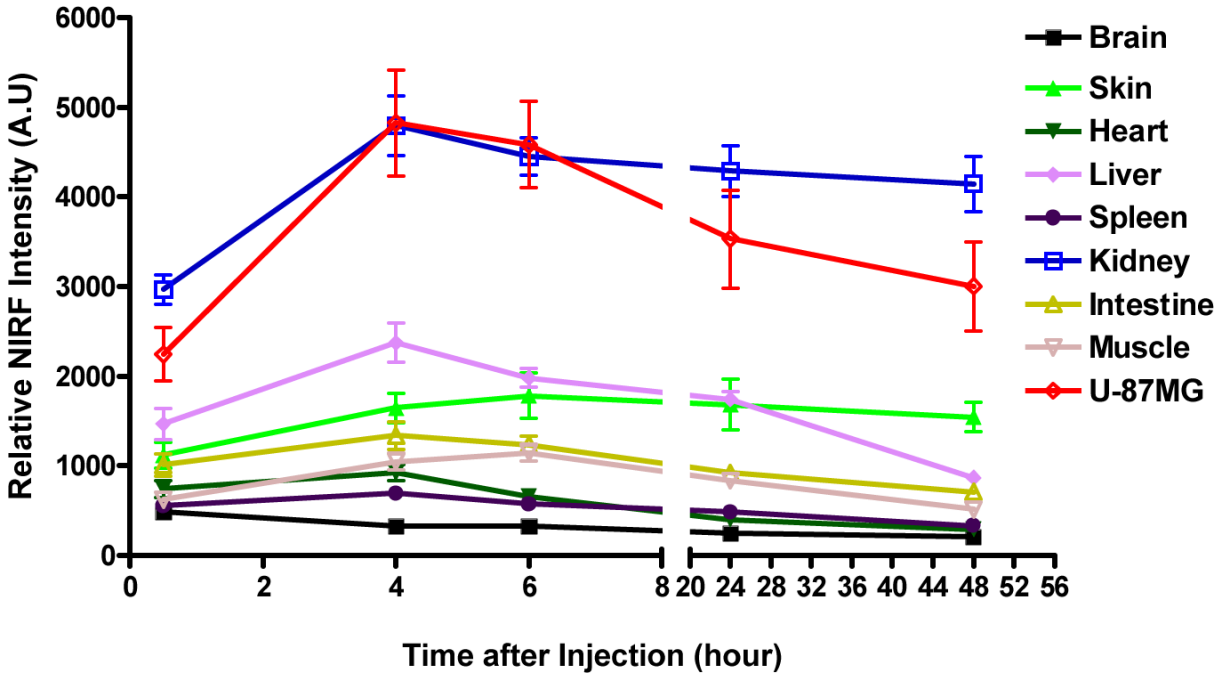

Figure 6a.

Biodistribution of the larger tetravalent LXY1-biotin-SA-Cy5.5 complex after injection into mice (n=3) bearing subcutaneous U-87 MG tumor. Near infrared fluorescent *ex vivo* imaging was conducted at 30min, 4hr, 6hr, 24hr, 48hr after injection of LXY1-biotin-SA-Cy5.5 (n=3 for each time point). NIRF signal in U-87MG tumor and kidneys peaked at around 4 hr after injection and majority of the signal remained even after 48 hr. NIRF uptake into the liver and skin are significant.

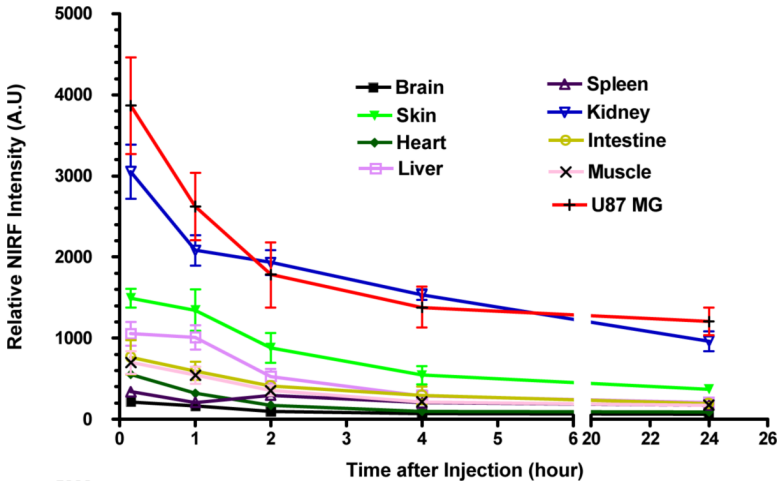

Figure 6b.

Biodistribution of the smaller univalent LXY1-Cy5.5 conjugate are injection into mice (n=3) bearing subcutaneous U-87MG tumor. Near infrared fluorescent *ex vivo* imaging were conducted at 15 min, 1 hr, 2 hr, 4 hr, 24 hr after injection of LXY1-Cy5.5. NIRF signals in the tumor and kidneys peaked at 15min followed by a rapid clearance within the first 4 hr and then a slow washout with significant retention of the NIRF probe in these two sites even after 24 hr. Liver and skin uptake was significant but the probe was cleared from these organs after 24 hr.